Photolytic degradation of molecular iodine adsorbed on model SiO2 particles

Alexandre Figueiredo, Rafal Strekowski, Loic Bosland, Amandine Durand, Henri Wortham

Photolytic degradation of molecular iodine adsorbed on model SiO$_2$ particles

A. Figueiredo [a,b], R.S. Strekowski [*,a], L. Bosland [b], A. Durand [a], H. Wortham [*, a]

[a] Aix Marseille Univ, CNRS, LCE, Marseille, France
[b] Institut de Radioprotection et de Sûreté Nucléaire, PSN-RES/SAG/LETR, Cadarache, France

Abstract

A molecular derivatization method followed by gas chromatographic separation coupled with mass spectrometric detection was used to study photolytic degradation of I$_2$ adsorbed on solid SiO$_2$ particles. This heterogeneous photodegradation of I$_2$ is studied at ambient temperature in synthetic air to better understand I$_2$ atmospheric dispersion and environmental fate. The obtained laboratory results show a considerably enhanced atmospheric lifetime of molecular iodine adsorbed on solid media. The heterogeneous atmospheric residence time (τ) of I$_2$ is calculated to be $\tau \approx 187$ minutes, i.e., $\tau \approx 3$ hours. The obtained heterogeneous lifetime of I$_2$ is shown to be considerably longer than its destruction by its principal atmospheric sink, namely, photolysis. The observed enhanced atmospheric lifetime of I$_2$ on heterogeneous media will likely have direct consequences on the atmospheric transport of I$_2$ that influences the toxicity or the oxidative capacity of the atmosphere.

Keywords:

Atmospheric reactivity; Molecular iodine; Heterogeneous reactivity; Photolysis; Kinetics; Silica particles

1. Introduction

More than 200 years after its discovery (Courtois, 1813), molecular iodine (I$_2$) continues to intrigue and challenge the scientific community to better understand and model its atmospheric fate and the reactivity of its oxidation products. To date, the atmospheric and environmental gas-phase I$_2$ emissions are well characterized. Natural ocean emissions account for the majority of the gas-phase I$_2$ atmospheric sources (Garland, 1967; Garland and Curtis, 1981; Saiz-Lopez et al., 2012) and the atmospheric mixing ratios of I$_2$ have been measured to vary from few pptv to 300±100 pptv (Bitter et al., 2005; Finley and Saltzman, 2008; Huang et al., 2010; Leigh et al., 2010; Mahajan et al., 2010, 2009; Peters et al., 2005; Saiz-Lopez et al., 2006; Saiz-Lopez and Plane, 2004). More recently, molecular iodine emissions have gained an increased interest in the scientific community and the executive branches of some governments following the major nuclear power plant accident in Fukushima (Japan) (Kinoshita et al., 2011). That is, it is known that molecular iodine could be one of the major contributors to the

source term in the environment after an accident when the reactor containment wall is breached or damaged or the containment venting procedure has been applied to relieve the pressure within the building. Also, radioactive gas-phase I_2 emissions from nuclear power plant installations are difficult to retain by post-accident filtration systems (Ball et al., 2011) and, therefore, may be readily released into the environment if a major accident were to occur.

Once released into the atmosphere, the environmental fate of molecular iodine is important because it plays a major role in the oxidative capacity of the troposphere (Bloss et al., 2005), aerosol formation and atmospheric ozone cycles (Davis et al., 1996; McFiggans et al., 2000) among others. Further, in case of radioiodine release from a nuclear powerplant, its dispersion and its chemical forms (gaseous/particulate) in the atmosphere need to be modeled to ensure the radioprotection of the population. The atmospheric fate of gas-phase molecular iodine is known to be governed mainly by photolysis and molecule-radical reactions with atmospheric oxidants that include hydroxyl radicals and oxygen atoms among others. On the other hand, the literature data that reports on the heterogeneous interactions of gas-phase I_2 is limited. This is problematic since heterogeneous media such as aerosols and particles are inherent and omnipresent in the atmospheric system and represent a colossal number of potential surfaces for gas-phase I_2 – solid/liquid interactions, a hypothesis that has been supported by early laboratory experiments (Chamberlain, 1960; Chamberlain and Chadwick, 1966; Gard et al., 1998; Shen et al., 2013) that show that gas-phase I_2 readily adsorbs on solid atmospheric particles. Further, the kinetics of gas-phase molecular iodine's interaction on solid surfaces may be very different from its reactivity in the homogeneous phase (Finlayson-Pitts and Jr, 1999). This difference may have a direct impact on the gas-phase I_2 atmospheric fate and lifetime and, therefore, its capacity to be transported over long distances (Garland, 1967; Megaw, 1965).

While gas-phase I_2 is now well known to contribute to the atmospheric particle formation (Saiz-Lopez et al., 2012), the literature is nonexistent or scant at best that reports on reactivity and reaction mechanisms of gas-phase I_2 adsorbed on solid particles under controlled conditions. As a result, the aim of this work is to study the influence a solid media may play on the photolytic gas-phase iodine reactivity. While the aim of this work is to study photolytic I_2 – solid surface reactivity of nuclear electric power plant safety interest, only stable iodine-127 isotope is studied. That is, the reactivity of the radioisotope iodine-131 is not considered because it is assumed that the reactivity is controlled by the available valence electrons. Since iodine-127 and iodine-131 have the same number of valence electrons, their reactivity is expected to be equivalent. Another parameter that may play a role in the reactivity is the kinetic isotope effect (KIE) resulting from slightly different molar masses of iodine. It is not believed that the kinetic isotope effect (KIE) resulting from the mass-dependence of collision frequencies plays a major role in the heterogeneous interactions of molecular iodine (Coenen et al., 2006; Deitz, 1987; Wahl and

Bonner, 1951). While the KIE has been shown to play a role in the homogeneous gas-phase kinetics of OH radicals with non-methane hydrocarbons containing C-12 and C-13 isotopes (Rudolph et al., 2002, 2000), this effect is relatively low (1‰ to ~16‰) for carbon isotopes (Cantrell et al., 1990; Rudolph et al., 2000). Also, the KIE is expected to decrease with increasing number of carbon atoms (or molecular mass) (Rudolph et al., 2000). Therefore, it is assumed that the KIE due to the small difference between molecular mass of iodine-127 and iodine-131 will be relatively low or negligible (Coenen et al., 2006; Deitz, 1987; Wahl and Bonner, 1951).

The experimental method developed and used to detect gas-phase I_2 adsorbed on solid particles is based on previous work that studied heterogeneous reactivity of ozone with selected semi-volatile organic compounds (Palm et al., 1999; Pflieger et al., 2011). Further, the analytical detection of molecular iodine adsorbed on solid surfaces used in this work is based on the experimental method proposed by Ho-Sang Shin et al (Shin et al., 1996) and Zhang et al (Zhang et al., 2010) who used a derivatization agent to detect molecular iodine and other iodine containing compounds in aqueous solutions. The experimental details that are relevant to this work are given below.

2. Experimental

Similar to the experimental method of Pflieger et al. (Pflieger et al., 2011), a 500 cm³ pure Pyrex bulb attached to a modified rotary evaporator (Laborota 4000 efficient, Heidolph) was used to study the heterogeneous adsorption of gas-phase molecular iodine on solid silica particles in the presence of solar radiation in the ultraviolet and visible region of the solar spectrum. The schematic representation of the experimental setup is shown in Figure 1. Under typical experimental conditions, about 500 mg of dried silica particles coated with molecular iodine was placed within the Pyrex bulb. The bulb was attached to the modified rotary evaporator and immersed in a temperature-controlled bath. The experimental bath temperature was T = (298±1) K. The Xenon Lamp 300W was used to serve as a photolytic light source to irradiate the sample within the Purex bulb. The bulb was allowed to rotate to ensure that the I_2-coated particles within the Pyrex bulb were well homogenized. This assured that all the particles were well exposed to UV and visible light.

A continuous flow of synthetic air (zero air generator) was allowed to enter the bulb volume. The total air flow was controlled using a mass flow controller and the total air mass flow was 250 sccm. Part of the main flow was diverted using a restriction needle valve and allowed to enter two bubblers placed in a series and filled with ultra-pure water to obtain the desired humidity. The relative humidity was measured directly in the gas flow using a hygrometer "Hygrolog NT2" (Rotronic) with "HygroClip SC04" probe. The instrument accuracy of relative

humidity measurements was ±1.5%. The measured temperature within the Pyrex bulb was T = (298±1)K and the experimental relative humidity was 40±1.5%

2.1. Particles

Since atmospheric particles vary both in their physical nature and chemical complexity, to better simulate heterogeneous reactivity on atmospheric aerosols in a laboratory setting the choice of particle type is crucial. In this work, AEROSIL R812 silica particles were used to study the photolytic degradation of molecular iodine (Mattei et al., 2019, 2018; Socorro et al., 2015). Of course, these commercial silica particles are model particles and are not necessarily representative of all the particles found in the real atmosphere. However, they were chosen because as much as 20 to 30% of inorganic particles found in the natural atmosphere have been estimated to be oxides that include SiO_2. The siloxane surface of the AEROSIL R812 silica particles is, therefore, a good first approximation of the inorganic oxide particle content found in the atmosphere and will assist the research community to better understand and predict the fate of molecular iodine on solid particles.

The AEROSIL R812 (Silanamine, 1,1,1-trimethyl-N-(trimethylsilyl)-, hydrolysis products with silica; CAS Number: 68909-20-6) was purchased from Evonic Degussa GmbH and the stated minimum SiO_2 content was ≥ 99.8%. AEROSIL R812 is a fumed silica after-treated with organosilane with high specific surface and marked hydrophobia. The stated specific surface area (based on Brunauer-Emmett-Teller (BET) analysis conducted at the boiling temperature of N_2, 77K) was 260 ± 30 m^2 g^{-1} (Evonic Degussa GmbH). The stated average particle size is 7 nm but the SiO_2 particles can agglomerate to form an aerosol of a few micrometers in diameter, mirroring suspended particles found in the atmosphere. Particle density was 50 g L^{-1}.

2.2. Particles coating

The SiO_2 particles were loaded using a liquid/solid adsorption method that has been reported previously (Mattei et al., 2019, 2018; Socorro, 2015; Socorro et al., 2015). To minimize any photo-degradation of molecular iodine, particle loading was performed in the dark. In a 500 cm^3 Pyrex bulb, 500 mg of silica particles were mixed with 100 mL of 9 mg L^{-1} solution of molecular iodine in cyclohexane (HPLC grade, ≥99.8%, Sigma-Aldrich) solution. The bulb and its contents were then placed in an ultrasonic bath for 15 minutes to homogenize the mixture. After, cyclohexane was removed under aspirator vacuum (Rotavapor R-114, Büchi) at T = 313 K and p = (256±20) mbar for 45 minutes. Assuming a uniform particle surface coverage for iodine molecules and a spherical particle geometry, the percentage of the particle surface coated with iodine was 0.2% of the monolayer for hydrophobic silica (Socorro et al., 2015).

4

2.3. Extraction and molecular iodine quantification

The extraction and quantification method used in this work to study the molecular iodine adsorption on SiO_2 particles is based on the analytical work performed by Ho-Sang Shin et al. (Shin et al., 1996) and Zhang et al. (Zhang et al., 2010). Similar to these authors' work, the 2,4,6-tribromoaniline internal standard and the N,N-dimethylaniline derivatization reagent were used to quantify molecular iodine present in a liquid solution. Under typical experimental conditions, 30 mg of the sample (SiO_2 particles coated with I_2) was extracted using a spatula from the Pyrex bulb every 30 minutes and placed in an air-tight vial (between 5 and 7 samples per experiment). The vial was then hermetically sealed and stored at T=-20°C for ≤24 hours. Following aliquoting, 50 μL of the internal standard and 50 μL of the 300 mg L^{-1} N,N-dimethylaniline solution in cyclohexane was added to the vial. After, the contents of the vial were placed in the 33 mL stainless-steel compartment volume of the Accelerated Solvent Extraction (ASE 300, Dionex) system. The optimized extraction conditions were the following: extraction solvent, cyclohexane; oven temperature, 100 °C; pressure, 100 bars; heat up time, 5 min; static time 5 min. The flush volume amounted to 150% of the extraction cell volume. The extracted analytes dissolved in cyclohexane were purged from the sample cell using pressurized nitrogen gas (p=100 bars) for 300 seconds. Three cycles per cell were performed. After, the extracts were concentrated under a flow of nitrogen gas using a concentration workstation (TurboVap II, Biotage) with 13 < p(psi) < 17 and T=323 K. The extracted solution was concentrated to a final volume of 500 μL. The obtained extract was filtered using a PTFE (0.22 μm pore size) membrane filter and then analyzed using the TRACE GC Ultra (Thermo Scientific) gas chromatography (GC) coupled to the TSQ Quantum Triple Quadrupole Mass Spectrometer (MS) (Thermo Scientific). A Thermo TG-5MS capillary column (Thermo Scientific, 30 m × 0.25 mm i.d., 0.25 μm) was used. The helium (99.999%, Air Liquide) carrier gas flow rate was 1 mL min^{-1}. One microliter (1 μL) liquid samples were injected in the splitless mode and the injector temperature was maintained at T = 493 K. The GC oven temperature was held at T=35 °C for one minute and then programmed at the rate of 30 °C min^{-1} to 220 °C and held for 11 minutes. The transfer line between the GC and the mass analyzer was maintained at T =280 °C. The tandem mass spectrometer (MS/MS) analyzer was operated in a full scan / single ion monitoring mode to increase the sensitivity. The electron impact (EI) ionization detector of the MS/MS system was operated at 70 eV ionization energy and the EI source temperature was T = 250°C.

3. Results and Discussion

Molecular iodine was not detected directly. That is, I_2 adsorbed on SiO_2 particles was allowed to react with the given derivatization agent, namely, N,N-dimethylaniline, in cyclohexane to form 4-iodo-N,N-dimehylaniline

(Mishra et al., 2000). The 4-iodo-N,N-dimethylaniline was then extracted in cyclohexane as described above and quantified using the GC-MS/MS technique. The extraction yield for 4-iodo-N,N-dimethylaniline was calculated to range from 65% to 75%. The N,N-dimethylaniline was added in excess and, therefore, it was assumed that the molecular iodine derivatization reaction was total (Mishra et al., 2000). That is, it is known that I_2 reacts to completion with N,N-dimethylaniline to form 4-iodo-N,N-dimethylaniline within minutes (Mishra et al., 2000). Similar to the work of Mishra et al. (Mishra et al., 2000), all reagents, namely N,N-dimethylaniline, 4-iodo-N,N-dimethylaniline and the 2,4,6-tribromoaniline internal standard were identified by comparison of GC retention times and mass spectra of control reagents. As stated above, the tandem mass analyzer was operated in a full scan / single ion monitoring mode to increase the sensitivity. The 4-iodo-N,N-dimethylaniline derivatization product was identified and quantified using the GC retention times and peak intensity at m/Q 247 and the 2,4,6-tribromoaniline internal calibrant was identified and quantified using the GC retention times and peak intensities at m/Q 330. A typical GC chromatograph and the total ion mass spectra is shown in Figure 2.

Molecular iodine concentration was calculated from the ratio of the iodine derivative product peak area to that of the 2,4,6-tribromoaniline internal standard peak area. The resulting typical calibration graph is shown in figure 3. The calibration plot shown in Figure 3 is an average of 5 independent experiments of the molecular iodine calibration results for iodine concentrations in the range from 5 to 40 mg L^{-1}. As shown in figure 3, the solid line is obtained from a least squares analysis and gives the following linear expression : $(2.51 \pm 0.05) \times 10^{-2}[I_2]$. Uncertainty is $\pm 1\sigma$ and represents precision only. The obtained correlation coefficient was 0.9879. The calculated limit of detection and limit of quantification were 0.21 mg L^{-1} and 0.63 mg L^{-1} for iodine, respectively. The uncertainty in the molecular iodine concentration measurements were evaluated using the error in weighing ± 0.1 mg, the repeatability of the weighing (student test) and the repeatability in the measurement of the I_2 concentration for the entire method (student test). The obtained uncertainty in the iodine measurement concentration adsorbed on silica particles was estimated to be $\pm$ 20%.

3.1. Rate of photolysis of I_2

The kinetics of the heterogeneous photolysis of molecular iodine on SiO_2 particles were determined by monitoring the loss of I_2 as a function of time. The photolysis of I_2 on SiO_2 particles exhibited an exponential decay, suggesting pseudo-first-order kinetics. However, the rate of loss of concentration of I_2 on solid surfaces is a process that must include both the photolysis and desorption phenomena.

$$\frac{d[I_2]}{dt} = -k_{obs}[I_2] = -(k_{desorption} + J)[I_2]$$

In the equation above, $k_{obs}(s^{-1})$ is the observed first-order rate constant, $k_{desorption}(s^{-1})$ is the desorption first-order rate constant, $J(s^{-1})$ is the photodissociation rate constant, $t(s)$ is the time of exposure to solar radiation and $[I_2]$ is the normalized iodine concentration adsorbed on the silica particles. The heterogeneous photolysis kinetics were determined by analyzing their corresponding temporal profiles in a time frame 0 to 3 h.

The 300 W Xenon lamp (LOT, Oriel) was used as a source of solar radiation to irradiate iodine adsorbed on SiO_2 particles within the Pyrex bulb volume. A spectroradiometer (SR-501, Spectral Evolution) equipped with an integrating sphere to account for any reflection was used to measure the spectral irradiance within the reactor under the exact experimental conditions. That is, to measure the Xe arc lamp irradiance, the SR-501 spectroradiometer was placed within the Pyrex bulb. As a result, the irradiance was measured across the Pyrex wall respecting the exact light path distances and environmental conditions of a given experiment. The average spectral irradiance of the Xe lamp (dotted line) is shown Figure 4. Further, the reference solar spectral irradiance (solid line) shown in Figure 4 was taken on 2019/09/05. In more detail, the reference solar spectral irradiance shown in figure 4 was measured using our SR-501 spectroradiometer equipped with the integrating sphere. This measurement was taken outside our laboratory under given atmospheric conditions (zero cloud cover, atmospheric conditions that are typical of Marseille, France, during the Mistral wind conditions) from 11 a.m. to 2 p.m. local time. The outdoor solar irradiance was measured in parallel (at the same time) with outdoor laboratory experiments carried out using a quartz reactor. In summary, the reference solar irradiance spectrum shown in Figure 4 corresponds to an averaged noon-time solar spectral irradiance for Marseille, France, (Latitude: 43.3, Longitude: 5.4). The I_2 absorption spectrum shown in Figure 4 was obtained using the UV-Visible spectrophotometer (Jasco V-670 spectrophotometer equipped with a horizontal integrating sphere PIN-757) under given experimental conditions. That is, molecular iodine surface coverage on SiO_2 particles was 0.2%. The UV-Visible spectrophotometer used to measure the absorbance of I_2 adsorbed on SiO_2 particles was operated in the absorbance mode $250 < \lambda(nm) < 800$. The scan rate was 200 nm.min^{-1} and the wavelength resolution was 0.2 nm.

The radiometric measurements shown in Figure 4 indicate that the solar spectrum does not strictly follow the Xe lamp spectral irradiance. It may be seen in Figure 4 that the Xe lamp irradiance goes "deeper" into the UV region of the solar spectrum than the obtained solar spectrum irradiance. That is, the solar radiation starts at $\lambda \sim 295$ nm while the observed Xe lamp emission within the reactor starts at $\lambda \sim 275$ nm. As shown in Figure 4, molecular

iodine absorbs in the region $280 < \lambda(nm) < 600$ nm of the solar spectrum with a maximum absorption value at $\lambda \sim 360$ nm.

3.2. Desorption of iodine adsorbed on SiO_2 particles

Since the vapor pressure of solid molecular iodine is about $p = 0.25 - 0.31$ mmHg (Baxter et al., 1907; Stull, 1947) at T=20°C, part of the initial I_2 concentration adsorbed on SiO_2 particles will certainly volatilize over time. To account for and to quantify this loss, experiments were carried out in the absence of light. A typical normalized iodine concentration temporal profile under dark conditions is shown in Figure 5. As shown in Figure 5, after 3 hours, the observed I_2 concentration is about $0.3 \times [I_2]_0$, where the $[I_2]_0$ is the initial molecular iodine concentration adsorbed on SiO_2 particles. The first-order desorption rate constant for I_2 adsorbed on SiO_2 particles is derived from the data and gives $k_{desorption} = (1.1 \pm 0.2) \times 10^{-5}$ s^{-1} (the calculated uncertainty is $\pm 1\sigma$).

3.3. Heterogeneous photolysis

To evaluate the kinetics of iodine photolysis adsorbed on SiO_2 particles, experiments were conducted in the presence of UV-Visible radiation. As stated before, the 300W high pressure xenon lamp was employed to irradiate the I_2/SiO_2 solid mixture. The irradiation time was three hours. Typical normalized iodine concentration temporal profiles for two different experiments carried out at T=298K and 40%RH following the photolysis of the I_2/SiO_2 solid mixtures are shown in Figure 6 to check the reproducibility. The first-order rate constants for the photolysis of the I_2/SiO_2 solid mixtures are derived from the data and give $k_{obs} = (8.2 \pm 0.1) \times 10^{-5}$ s^{-1} and $k_{obs} = (1.2 \pm 0.2) \times 10^{-4}$ s^{-1} (the calculated uncertainties are $\pm 1\sigma$).

To obtain the photodissociation rate constant, J, for I_2 adsorbed on SiO_2 particles, the obtained desorption rate constant, $k_{desorption}$, is subtracted from the observed photolysis rate constant, k_{obs}. The resulting average photodissociation rate constant, J, for I_2 adsorbed on SiO_2 particles, is calculated to be $J = (8.9 \pm 1.1) \times 10^{-5}$ s^{-1}. The k_{obs} and $k_{desorbtion}$ may depend on the gas flow rate going through the reactor. However, as the J value is calculated by the difference in the two parameters, since the gas flow rates are the same (among other experimental conditions), it is assumed that J value does not depend on the gaz vector flow rate.

As shown in Figure 4, the solar spectrum does not strictly follow the Xe lamp spectral irradiance. More precisely, the solar radiation irradiance starts at $\lambda \sim 300$ nm while the observed Xe lamp irradiance starts at $\lambda \sim 280$ nm. To account for this difference and to better approach the real-life experimental conditions, additional heterogeneous photolysis experiments were carried out using a quartz reactor and real sun light as the radiation source. It is known

that cultured quartz transmits light $\lambda>147$ nm, a wavelength value that is well beyond the Pyrex glass transmission properties (cutoff at $\lambda\sim300$ nm).

Typical normalized iodine concentration temporal profiles for experiments carried out under dark and light conditions using a quartz reactor and natural solar radiation as a light source are shown in figure 7b. The reproducibility of the test in presence of solar radiation was performed (Figure 7c).

As shown in Figure 7, the first-order desorption rate constants for I_2 adsorbed on SiO_2 particles in the absence of solar radiation is derived from the data to give $k_{desorption} = (1.1 \pm 0.2) \times 10^{-5}$ s^{-1}. The first-order rate constants for the photolysis of the I_2/SiO_2 solid mixtures within a quartz reactor are derived from the data and give $k_{obs} = (2.4 \pm 0.3) \times 10^{-4}$ s^{-1} and $k_{obs} = (2.2 \pm 0.2) \times 10^{-4}$ s^{-1}. All uncertainties are $\pm 1\sigma$. Similar to the situation listed above, the photodissociation rate constant, J, for I_2 adsorbed on SiO_2 particles, is obtained from the difference of the $k_{desorption}$ and k_{obs}. The resulting average photodissociation rate constant, J, for I_2 / SiO_2 particle photolysis carried out in a quartz reactor and using direct sunlight photolysis, is calculated to be $J = (2.2 \pm 0.3) \times 10^{-4}$ s^{-1}.

4. Conclusion and Atmospheric Implications

A molecular derivatization method followed by GC separation coupled with MS/MS detection was used to study photolytic degradation of I_2 on model SiO_2 solid particles. The heterogeneous photodegradation of I_2 was studied at ambient temperature at 40%RH in synthetic air to better understand its atmospheric dispersion and environmental fate. The average photodissociation rate constant on model particles is calculated to be $J = (8.9 \pm 1.1) \times 10^{-5}$ s^{-1} at T=298K. The resulting heterogeneous atmospheric residence time (τ) of I_2 is calculated to be $\tau\approx187$ minutes, i.e., $\tau\approx3$ hours. The resulting average photodissociation rate constant using real solar radiation light source is calculated to be $J = (2.2 \pm 0.3) \times 10^{-4}$ s^{-1}. This value is slightly more than twice the measured estimate of the rate constant obtained using the Xe lamp photolytic light source. However, given the same order of magnitude of the two rate constants, we conclude that the choice of a photolytic radiation source has only a small effect on the studied heterogeneous photolysis under given experimental conditions. The obtained heterogeneous residence time of I_2 is considerably greater compared to other atmospheric destruction pathways of gas-phase I_2, namely, photolysis and radical-I_2 reactions of atmospheric interest. It is known that photolysis is the principal atmospheric sink of gas-phase I_2 and the photolytic residence time of gas-phase I_2 is reported to be $\tau \approx 10$ seconds (Saiz-Lopez et al., 2012); a value that is 1000 times lower that the heterogeneous lifetime value of I_2 reported in this work. The observed difference between the photolytic lifetime and the heterogeneous one may

9

potentially be explained through several phenomena. One, there may be considerable shielding of the light by the particles themselves. That is, iodine molecules may potentially be adsorbed on sites of the silica particles not accessible or little accessible to light. Two, part of the actinic flux may also be absorbed by the silica particles themselves. Three, there may also be considerable scattering of the light by the particles. However, at this point we are not able to definitely explain the observed difference in the two values. Clearly, this great experimental issue should be explored further. However, the physical processes governing the photolytic behavior of particles under given experimental conditions are likely to be similar to the ones observed in the natural atmosphere. That is, atmospheric particles will shield and "protect" the adsorbed species from sunlight. The atmospheric gas-phase molecular I_2 concentration has been measured to vary from 2.46×10^8 to 7.38×10^9 molecules cm^{-3} (Bitter et al., 2005; Finley and Saltzman, 2008; Huang et al., 2010; Leigh et al., 2010; Mahajan et al., 2010, 2009; Peters et al., 2005; Saiz-Lopez et al., 2006; Saiz-Lopez and Plane, 2004). However, I_2 adsorbed on solid atmospheric particles has not been studied in detail. That is, while much atmospheric research effort has been focused on speciation of different iodine radical compounds adsorbed on atmospheric particles, only one study reports on the total iodine that includes gas-phase I_2 adsorbed on aerosols (Baker et al., 2000). These authors (Baker et al., 2000) report the total iodine concentration (I_2, IO_3^-, IO ...) adsorbed on atmospheric particles in a coastal site in the southeast of England to be $\approx 2 \times 10^7$ molecules cm^{-3} (Baker et al., 2000). Consequently, it may be estimated that the ratio of total iodine adsorbed on atmospheric aerosols to the gas-phase I_2 concentration is not negligible ($\approx 0.3 - 10\%$). The obtained enhanced atmospheric lifetime of I_2 on heterogeneous media will likely have direct consequences on the atmospheric transport properties of I_2 that may influence the oxidative capacity of the atmosphere and the ratio between the gaseous and particulate iodine atmospheric loading. Given the observed enhanced heterogeneous residence time, I_2 adsorbed on solid particles has the capacity to be transported over longer distances than previously thought, a fact that may potentially modify current forecasts on the atmospheric transport of I_2.

In this work, I_2 release rate from SiO_2 particles under the photolysis effect has been quantified for the first time. The obtained results will help to improve the calculation of the evolution of iodine partition (between particulate and gaseous iodine) and iodine dispersion in the atmosphere. More generally, the obtained results will help the industrial and academic communities to better understand and predict the environmental fate of I_2 on aerosols. However, to better understand and model real-atmosphere heterogeneous behavior of I_2, other surfaces need to be included in the study of I_2-surface interactions that better represent and reflect the complex physical and chemical nature of particles found in the real environment.

References

Baker, A.R., Thompson, D., Campos, M.L.A.M., Parry, S.J., Jickells, T.D., 2000. Iodine concentration and availability in atmospheric aerosol. Atmospheric Environment 34, 4331–4336. https://doi.org/10.1016/S1352-2310(00)00208-9

Ball, J., Glowa, G., Boulianne, D., Mitchell, J., 2011. Behaviour of Iodine Project: Final Report on Organic Iodide Studies. Nuclear Energy Agency, Atomic Energy of Canada Limited: Chalk River, Ontario, Canada.

Baxter, G.P., Hickey, C.H., Holmes, W.C., 1907. THE VAPOR PRESSURE OF IODINE. J. Am. Chem. Soc. 29, 127–136. https://doi.org/10.1021/ja01956a004

Bitter, M., Ball, S.M., Povey, I.M., Jones, R.L., 2005. A broadband cavity ringdown spectrometer for in-situ measurements of atmospheric trace gases. Atmospheric Chemistry and Physics 5, 2547–2560.

Bloss, W.J., Lee, J.D., Johnson, G.P., Sommariva, R., Heard, D.E., Saiz-Lopez, A., Plane, J.M.C., McFiggans, G., Coe, H., Flynn, M., Williams, P., Rickard, A.R., Fleming, Z.L., 2005. Impact of halogen monoxide chemistry upon boundary layer OH and HO2 concentrations at a coastal site. Geophysical Research Letters 32. https://doi.org/10.1029/2004GL022084

Cantrell, C.A., Shetter, R.E., McDaniel, A.H., Calvert, J.G., Davidson, J.A., Lowe, D.C., Tyler, S.C., Cicerone, R.J., Greenberg, J.P., 1990. Carbon kinetic isotope effect in the oxidation of methane by the hydroxyl radical. Journal of Geophysical Research: Atmospheres 95, 22455–22462. https://doi.org/10.1029/JD095iD13p22455

Chamberlain, A.C., 1960. Aspects of the deposition of radioactive and other gases and particles. Intern. J. Air Pollution 3.

Chamberlain, A.C., Chadwick, R.C., 1966. Transport of iodine from atmosphere to ground. Tellus 18, 226–237. https://doi.org/10.3402/tellusa.v18i2-3.9676

Coenen, H.H., Mertens, J., Mazieère, B., 2006. Radiation Reactions For Pharmaceuticals. Compedium for Effective Synthesis Strategies. Springer Netherlands.

Courtois, B., 1813. Découverte d'une substance nouvelle dans le Vareck. Annales de Chimie 304.

Davis, D., Crawford, J., Liu, S., McKeen, S., Bandy, A., Thornton, D., 1996. Potential impact of iodine on tropospheric levels of ozone. Journal of Geophysical Research 101, 2135–2147.

Deitz, V.R., 1987. Interaction of radioactive iodine gaseous species with nuclear-grade activated carbons. Carbon 25, 31–38. https://doi.org/10.1016/0008-6223(87)90037-6

Finlayson-Pitts, B.J., Jr, J.N.P., 1999. Chemistry of the Upper and Lower Atmosphere: Theory, Experiments, and Applications. Academic Press.

Finley, B.D., Saltzman, E.S., 2008. Observations of Cl$_2$, Br$_2$, and I$_2$ in coastal marine air. J. Geophys. Res. 113, D21301. https://doi.org/10.1029/2008JD010269

Gard, E.E., Kleeman, M.J., Gross, D.S., Hughes, L.S., Allen, J.O., Morrical, B.D., Fergenson, D.P., Dienes, T., E. Gälli, M., Johnson, R.J., Cass, G.R., Prather, K.A., 1998. Direct Observation of Heterogeneous Chemistry in the Atmosphere. Science 279, 1184. https://doi.org/10.1126/science.279.5354.1184

Garland, J.A., 1967. The adsorption of iodine by atmospheric particles. Journal of Nuclear Energy 21, 687–700. https://doi.org/10.1016/0022-3107(67)90106-2

Garland, J.A., Curtis, H., 1981. Emission of iodine from the sea surface in the presence of ozone. Journal of Geophysical Research: Oceans 86, 3183–3186. https://doi.org/10.1029/JC086iC04p03183

Huang, R.-J., Seitz, K., Buxmann, J., Pöhler, D., Hornsby, K.E., Carpenter, L.J., Platt, U., Hoffmann, T., 2010. In situ measurements of molecular iodine in the marine boundary layer: the link to macroalgae and the implications for O$_3$, IO, OIO and NO$_x$. Atmos. Chem. Phys. 10, 4823–4833. https://doi.org/10.5194/acp-10-4823-2010

Kinoshita, N., Sueki, K., Sasa, K., Kitagawa, J., Ikarashi, S., Nishimura, T., Wong, Y.-S., Satou, Y., Handa, K., Takahashi, T., others, 2011. Assessment of individual radionuclide distributions from the Fukushima nuclear accident covering central-east Japan. Proceedings of the National Academy of Sciences 108, 19526–19529.

Leigh, R.J., Ball, S.M., Whitehead, J., Leblanc, C., Shillings, A.J.L., Mahajan, A.S., Oetjen, H., Lee, J.D., Jones, C.E., Dorsey, J.R., Gallagher, M., Jones, R.L., Plane, J.M.C., Potin, P., McFiggans, G., 2010. Measurements and modelling of molecular iodine emissions, transport and photodestruction in the coastal region around Roscoff. Atmos. Chem. Phys. 10, 11823–11838. https://doi.org/10.5194/acp-10-11823-2010

Mahajan, A.S., Oetjen, H., Saiz-Lopez, A., Lee, J.D., McFiggans, G.B., Plane, J.M.C., 2009. Reactive iodine species in a semi-polluted environment. Geophys. Res. Lett. 36, L16803. https://doi.org/10.1029/2009GL038018

Mahajan, A.S., Plane, J.M.C., Oetjen, H., Mendes, L., Saunders, R.W., Saiz-Lopez, A., Jones, C.E., Carpenter, L.J., McFiggans, G.B., 2010. Measurement and modelling of tropospheric reactive halogen species over the tropical Atlantic Ocean. Atmospheric Chemistry and Physics 10, 4611–4624.

Mattei, C., Wortham, H., Quivet, E., 2019. Heterogeneous degradation of pesticides by OH radicals in the atmosphere: Influence of humidity and particle type on the kinetics. Science of The Total Environment 664, 1084–1094. https://doi.org/10.1016/j.scitotenv.2019.02.038

Mattei, C., Wortham, H., Quivet, E., 2018. Heterogeneous atmospheric degradation of pesticides by ozone: Influence of relative humidity and particle type. Science of The Total Environment 625, 1544–1553. https://doi.org/10.1016/j.scitotenv.2018.01.049

McFiggans, G., Plane, J.M.C., Allan, B.J., Carpenter, L.J., Coe, H., O'Dowd, C., 2000. A modeling study of iodine chemistry in the marine boundary layer. J. Geophys. Res. 105, 14371–14385. https://doi.org/10.1029/1999JD901187

Megaw, W.J., 1965. THE ADSORPTION OF IODINE ON ATMOSPHERIC PARTICLES. Pergamon Press Ltd.

Mishra, S., Singh, V., Jain, A., Verma, K.K., 2000. Determination of iodide by derivatization to 4-iodo-N,N-dimethylaniline and gas chromatography–mass spectrometry. Analyst 125, 459–464. https://doi.org/10.1039/A908363D

Palm, W.-U., Elend, M., Krüger, H.-U., Zetzsch, C., 1999. Atmospheric degradation of a semivolatile aerosol-borne pesticide: Reaction of OH with pyrifenox (an Oxime-Ether), adsorbed on SiO2. Chemosphere 38, 1241–1252. https://doi.org/10.1016/S0045-6535(98)00524-4

Peters, C., Pechtl, S., Stutz, J., Hebestreit, K., Honninger, G., Heumann, K.G., Schwarz, A., Winterlik, J., Platt, U., 2005. Reactive and organic halogen species in three different European coastal environments. Atmos. Chem. Phys. 19.

Pflieger, M., Grgić, I., Kitanovski, Z., Nieto, L., Wortham, H., 2011. The heterogeneous ozonation of pesticides adsorbed on mineral particles: Validation of the experimental setup with trifluralin. Atmospheric Environment 45, 7127–7134. https://doi.org/10.1016/j.atmosenv.2011.09.031

Rudolph, J., Czuba, E., Huang, L., 2000. The stable carbon isotope fractionation for reactions of selected hydrocarbons with OH-radicals and its relevance for atmospheric chemistry. Journal of Geophysical Research: Atmospheres 105, 29329–29346. https://doi.org/10.1029/2000JD900447

Rudolph, J., Czuba, E., Norman, A.L., Huang, L., Ernst, D., 2002. Stable carbon isotope composition of nonmethane hydrocarbons in emissions from transportation related sources and atmospheric observations in an urban atmosphere. Atmospheric Environment 36, 1173–1181. https://doi.org/10.1016/S1352-2310(01)00537-4

Saiz-Lopez, A., Plane, J.M.C., 2004. Novel iodine chemistry in the marine boundary layer. Geophysical Research Letters 31, 1999–2002. https://doi.org/10.1029/2003GL019215

Saiz-Lopez, A., Plane, J.M.C., Baker, A.R., Carpenter, L.J., von Glasow, R., Gómez Martín, J.C., McFiggans, G., Saunders, R.W., 2012. Atmospheric Chemistry of Iodine. Chem. Rev. 112, 1773–1804. https://doi.org/10.1021/cr200029u

Saiz-Lopez, A., Shillito, J.A., Coe, H., Plane, J.M.C., 2006. Measurements and modelling of I2, IO, OIO, BrO and NO3 in the mid-latitude marine boundary layer. Atmos. Chem. Phys. 16.

Shen, X., Zhao, Y., Chen, Z., Huang, D., 2013. Heterogeneous reactions of volatile organic compounds in the atmosphere. Atmospheric Environment 68, 297–314. https://doi.org/10.1016/j.atmosenv.2012.11.027

Shin, H.-S., Oh-Shin, Y.-S., Kim, J.-H., Ryu, J.-K., 1996. Trace level determination of iodide, iodine and iodate by gas chromatography-mass spectrometry. Journal of Chromatography A 732, 327–333. https://doi.org/10.1016/0021-9673(95)01281-8

Socorro, J., 2015. Etude de la réactivité hétérogène de pesticides adsorbés sur des particules modèles atmosphériques : cinétiques et produits de dégradation. http://www.theses.fr.

Socorro, J., Gligorovski, S., Wortham, H., Quivet, E., 2015. Heterogeneous reactions of ozone with commonly used pesticides adsorbed on silica particles. Atmospheric Environment 100, 66–73. https://doi.org/10.1016/j.atmosenv.2014.10.044

Stull, D.R., 1947. Vapor Pressure of Pure Substances. Organic and Inorganic Compounds. Ind. Eng. Chem. 39, 517–550. https://doi.org/10.1021/ie50448a022

Wahl, A.C., Bonner, N.A., 1951. Radioactivity Applied to Chemistry. Soil Science 72, Pp. 604.

Zhang, S., Schwehr, K.A., Ho, Y.F., Xu, C., Roberts, K.A., Kaplan, D.I., Brinkmeyer, R., Yeager, C.M., Santschi, P.H., 2010. A novel approach for the simultaneous determination of iodide, iodate and organo-iodide for 127I and 129I in environmental samples using gas chromatography-mass spectrometry. Environmental Science and Technology 44, 9042–9048. https://doi.org/10.1021/es102047y
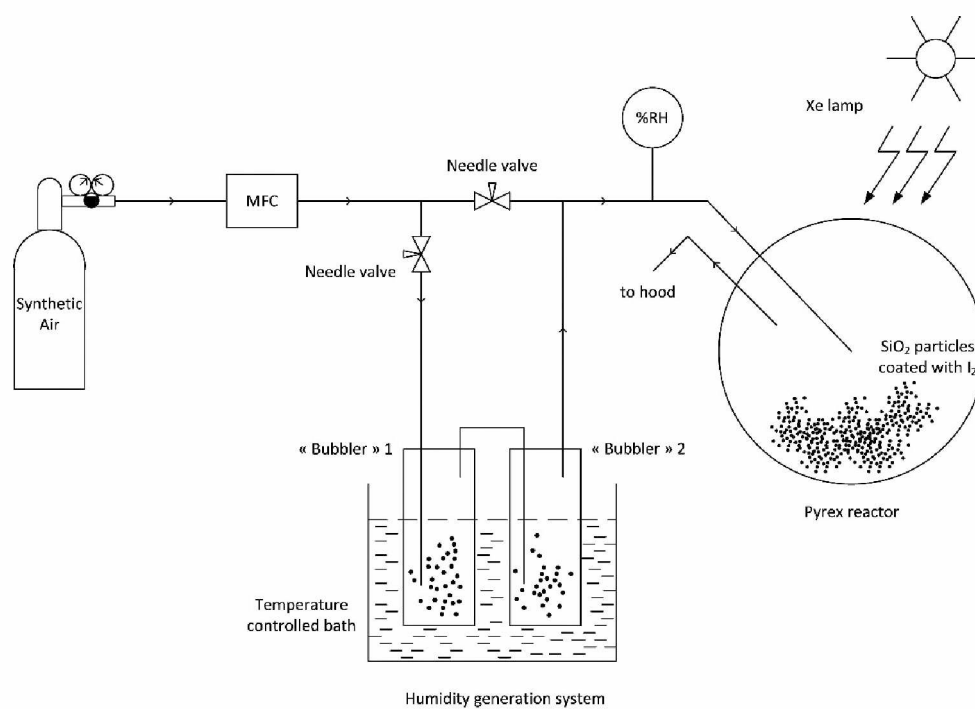
Figure 1. Schematic representation of the experimental system used to study the photolytic degradation of molecular iodine adsorbed on silica particles. MFC: Mass Flow Controler
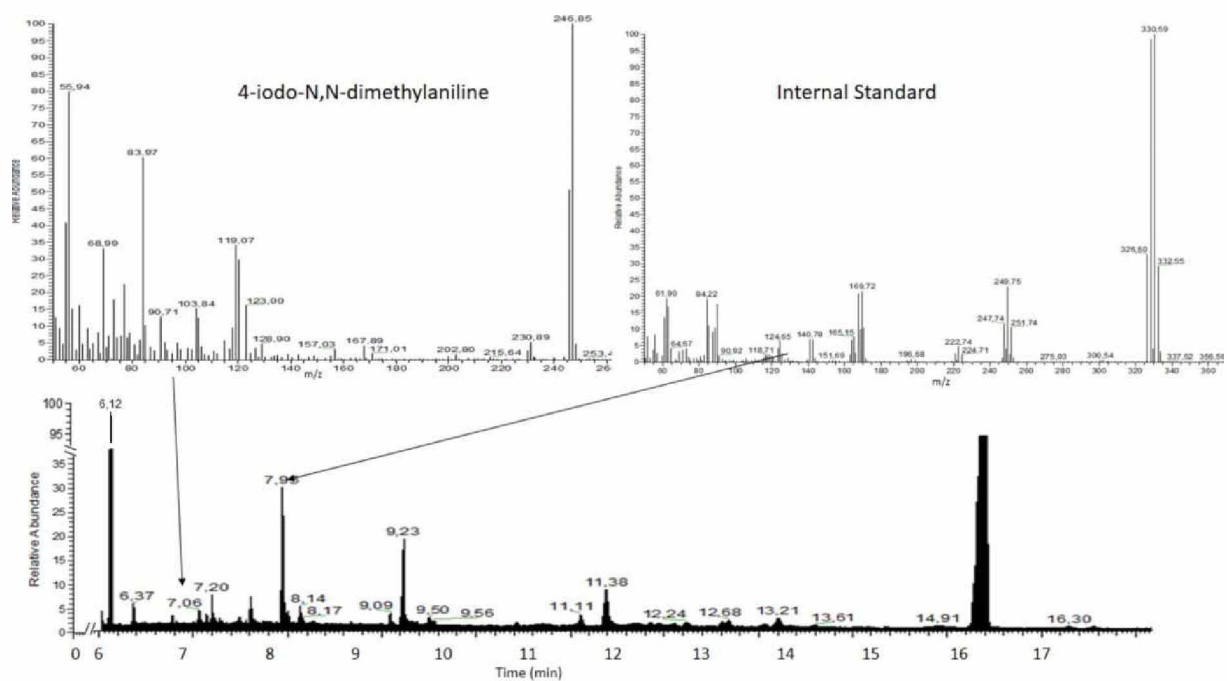
Figure 2. A typical GC chromatograph and the selected 4-iodo-N,N-dimethylaniline and internal standard total ion

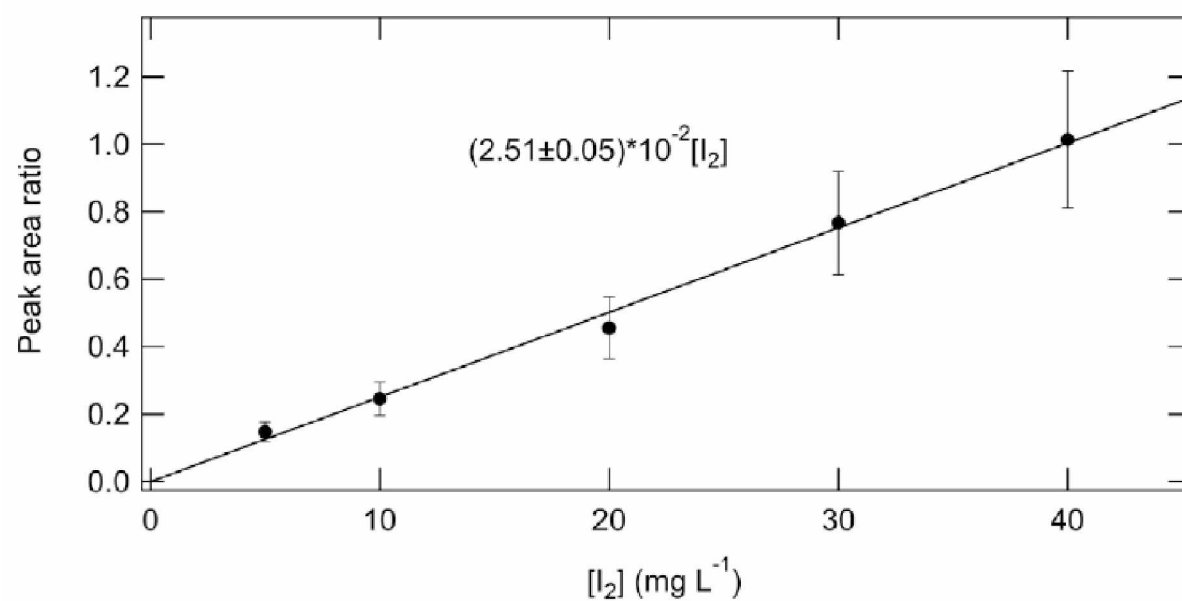MS spectra. Experimental conditions: [I2] = 12.2 mg/L; [2,4,6-tribromoaniline] =30 mg/L ; T =25 °C, 40%RH.

Figure 3. An average plot based on 5 independent experiments of the molecular iodine calibration results. The solid line is obtained from a least squares analysis and gives the expression shown in the figure. Errors are ±1σ, calculated fractional uncertainty. Experimental conditions: T=25°C, 40%RH.
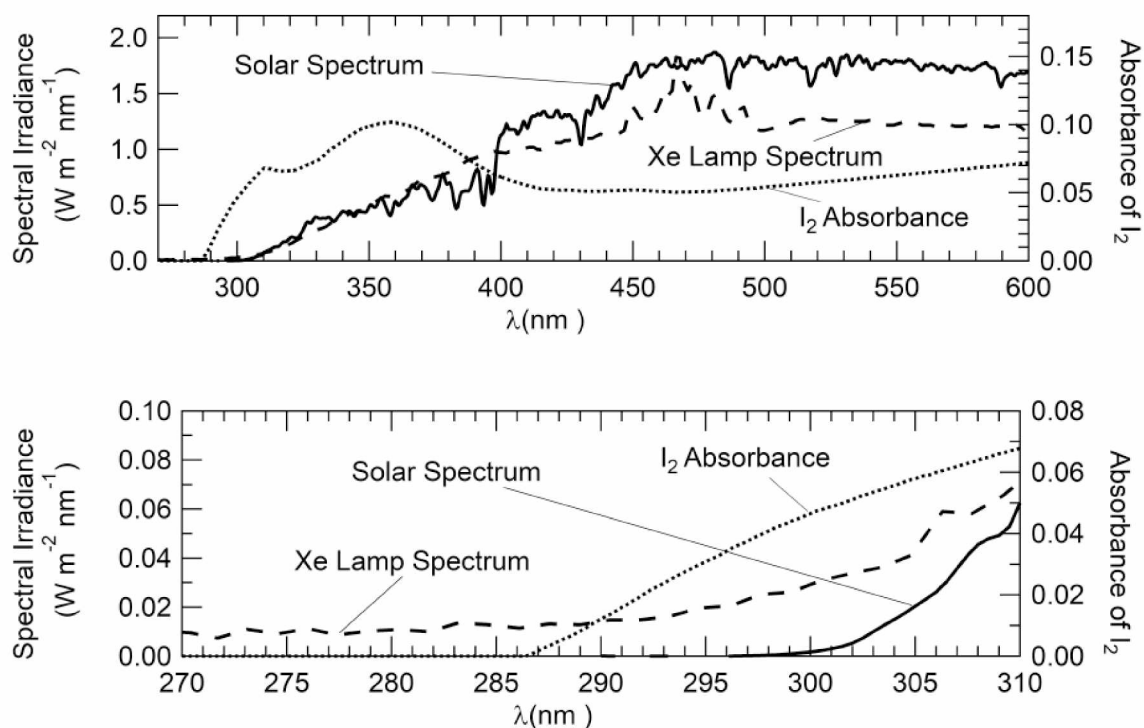
Figure 4. Comparison of the reference solar spectral irradiance (solid line) for Marseille, France 2019/05/05, (Latitude: 43.3, Longitude: 5.4), the 300W high pressure xenon lamp emission spectrum (dashed line) used to carry out the photolysis experiments and the average absorption spectrum of I2 (dotted line) adsorbed on SiO2 particles. The average I2 surface coverage was estimated to be 0.2%.
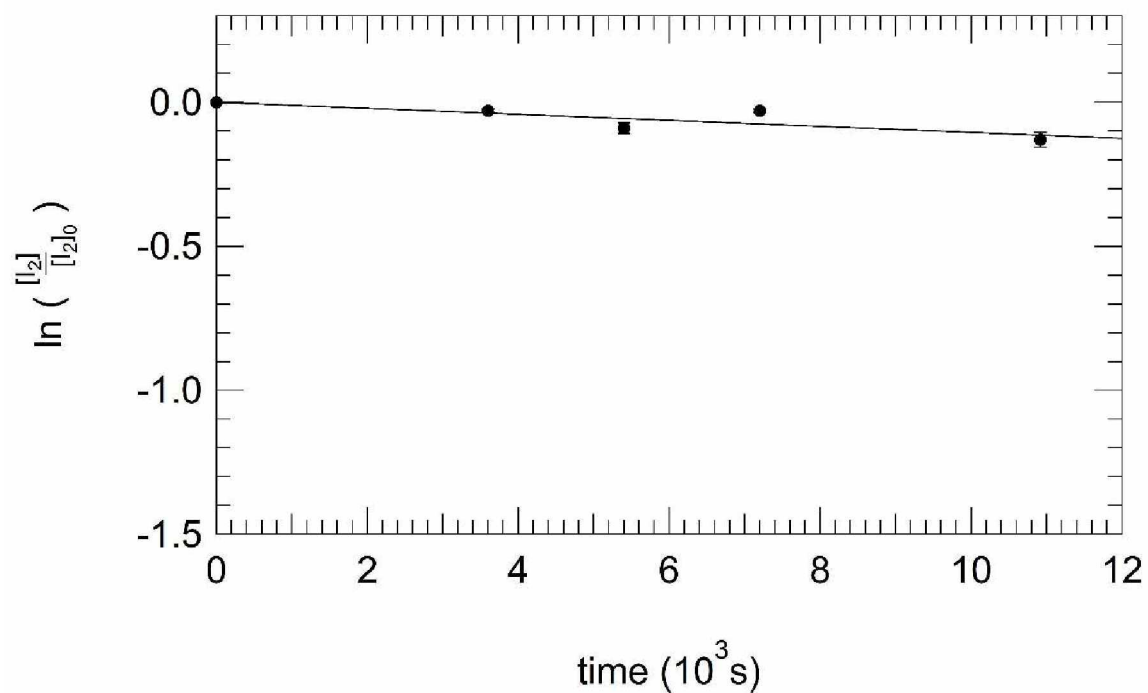
Figure 5. Typical normalized iodine concentration temporal profile in the absence of light (dark conditions). The solid line is obtained from a least squares analysis and gives. Error is ±1σ, precision only. Experimental conditions: T=298K; 40%RH; air flow = 250 mL min-1.
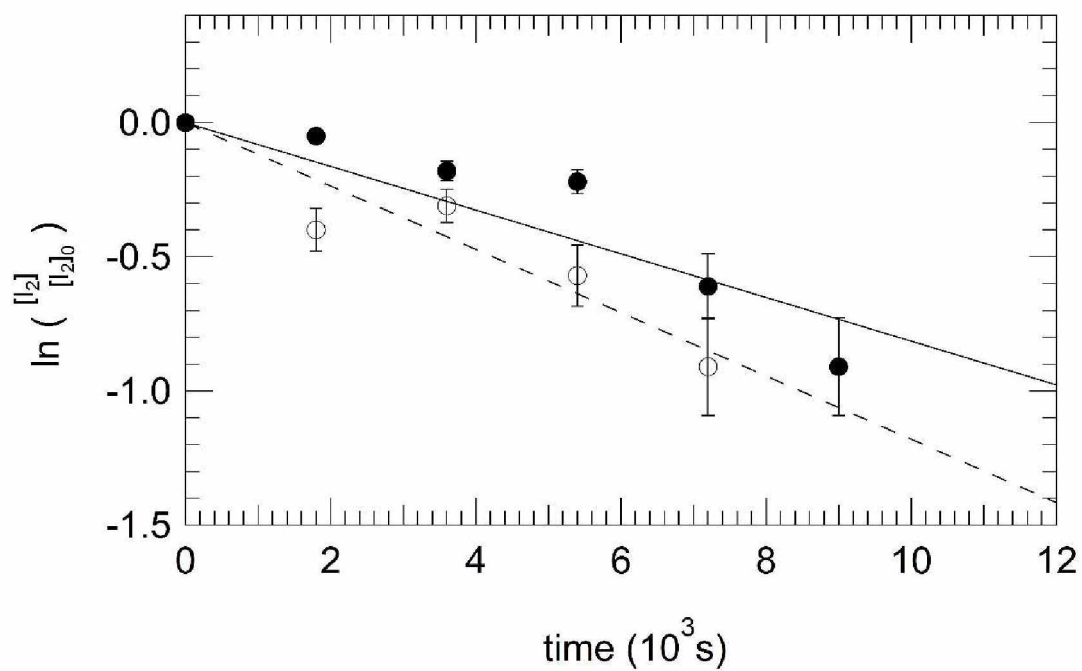
Figure 6. Typical normalized iodine concentration temporal profiles for two different experiments carried out under the same experimental conditions following photolysis of the I2 adsorbed on SiO2 particles. The solid and dashed lines are obtained from least squares analyses and give   (solid line) and   (dashed line) Errors are ±1σ, precision only. Experimental conditions: T=298K; 40%RH; air flow = 250 mL min-1; Xe lamp on.
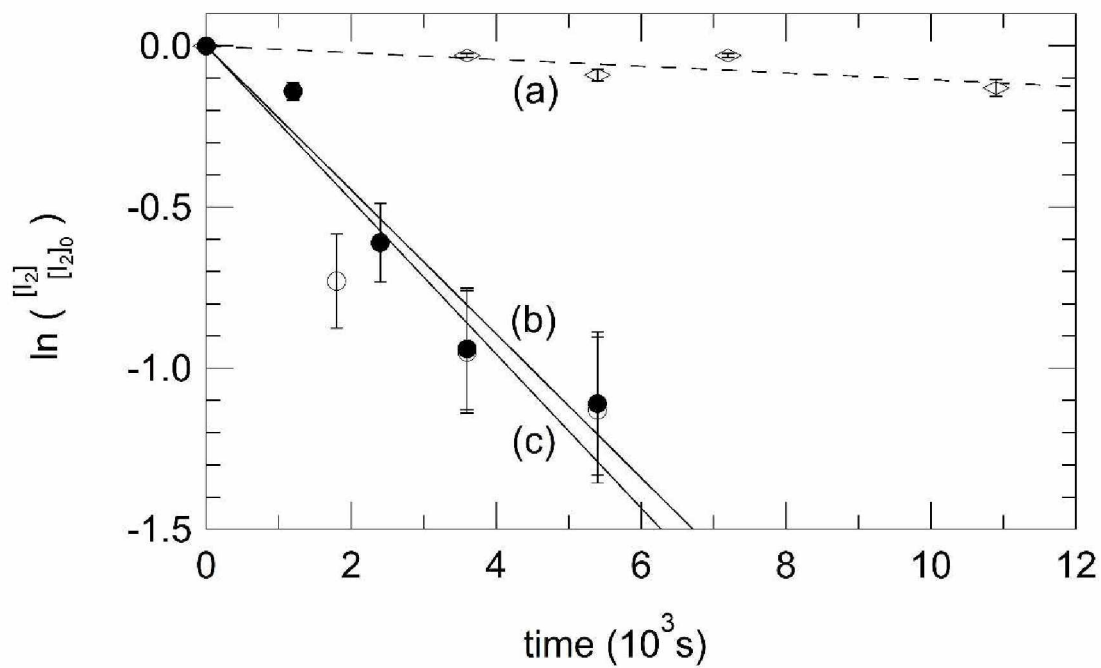
Figure 7. Typical normalized iodine concentration decay profiles carried out at T=298K in a quartz reactor and using natural sun light as the radiation source. Experiment (a) was carried out in the absence of solar radiation (dark conditions) and experiments (b) and (c) were carried out in the presence of solar radiation. Fits are obtained from linear least squares analyses and give the following first-order constants: (a) , (b) , and (c). Errors are ±1σ, precision only. Experimental conditions: T=298K, 40%RH, air flow = 250 mL min-1.